MENDES, M. & DE POLIGNAC, C. (1973). *Acta Cryst.* A**29**, 1–9.
ROLLETT, J. S. (1970). *Crystallographic Computing*, edited by F. R. AHMED, pp. 167–181. Copenhagen: Munksgaard.
RUDIN, W. (1964). *Principles of Mathematical Analysis*. New York: McGraw-Hill.
SINGH, A. K. & RAMASESHAN, S. (1966). *Acta Cryst.* **21**, 279–280.
SMITH, A. F. M. (1973). *J. R. Stat. Soc. B*, **35**, 67–75.
SRINIVASAN, R. (1966). *Z. Kristallogr.* **126**, 175–181.
STEIN, C. (1956). *Proc. 3rd Berkeley. Symp.*, Vol. 1, pp. 197–206.
TICKLE, I. (1975). *Acta Cryst.* B**31**, 329–331.
WASER, J. (1963). *Acta Cryst.* **16**, 1091–1094.
WEBB, G. I. (1974). Symposium on Bayesian Methods in Crystallography, Oxford. Unpublished paper.

Acta Cryst. (1978). A**34**, 738–743

Diffraction by Crystals with Planar Faults. III. Structure Analyses Using Microtwins

BY J. M. COWLEY AND ANDREW Y. AU

Department of Physics, Arizona State University, Tempe, Arizona 85281, *USA*

(*Received* 27 *November* 1977; *accepted* 23 *March* 1978)

The general theory for kinematical diffraction from crystals having planar faults is applied to the case of microtwinning and the related cases occurring in some minerals where there is a disordered sequence of two types of structure having small differences in composition, unit-cell dimensions and axial orientations. It is shown that, if intensities are measured for unresolved or partially resolved pairs of diffraction spots using conventional techniques, errors may well arise if the measurements are interpreted on the usual assumption that the intensities from the different crystal regions are summed incoherently. Calculations for representative cases suggest that errors, due to the neglect of the spreading of intensity maxima into continuous streaks, may amount to 20 or 30% when overlapping diffraction spots have structure amplitudes of opposite sign, but are usually much smaller, especially if the structure amplitudes are of the same sign.

In the first paper of this series [(Cowley, 1976*a*, hereinafter referred to as (I)] a general theory for kinematical diffraction from crystals having planar faults was presented. Applications to particular types of faults were given there and in the second paper of this series (Cowley, 1976*b*). These applications should be sufficient to illustrate the derivation of expressions appropriate to special cases from the general theory and it is not our intention to multiply examples. However in the course of discussions with Drs Gabrielle and J. D. H. Donnay on the interpretation of electron diffraction patterns from feldspars the question was raised as to the influence of microtwinning on the intensities which would be measured and used in the course of an X-ray diffraction structure analysis. We have therefore considered an idealized case of this kind and attempted to estimate the magnitude of any errors which might result from the application of accepted practices of structure analysis.

There are many cases reported in the literature for which it appears that twin planes occur more or less at random and, on the average only a few unit cells apart. One case, illustrated graphically by high-resolution electron microscopy, is that of monoclinic enstatite (Iijima & Buseck, 1976). In this case the two orientations of the monoclinic *a* axis differ by a sufficiently large angle to allow most pairs of related diffraction spots to be clearly separated, although there is considerable diffuse streaking intensity between them.

For some of the feldspars the separation of axial orientations may be very much smaller. The evidence of variation of axial orientations is not clear from diffraction patterns but may be deduced from the irregular mottling of electron-microscope images (the 'tweed' structure). For bytownite (McLaren & Marshall, 1974) the variation in orientation of the unit-cell axes over distance of the order of 100 Å appears to accompany compositional variations associated with an exsolution process. Similar orientational variations appear to be present in a Himalaya mine orthoclase (Prince, Donnay & Martin, 1973), giving rise to a tweed structure in high-resolution electron micrographs (Iijima, private communication), but it is not clear whether a compositional variation is involved in this case.

For convenience we continue our discussion in terms of 'twins', but the treatment will not exclude such cases involving variations of composition as well as small

variations of unit-cell dimensions and axial orientations where no twin relation between the two (or more) components is involved.

It is commonly assumed that the intensities of X-ray diffraction patterns from twins will be the sum of the intensity contributions from the orientations present. Even when spots from two orientations overlap or coincide it is assumed that the measured intensity from the joint peak will be $p|F_1|^2 + q|F_2|^2$ where F_1 and F_2 are the structure amplitudes of the two types of unit cell and p and q are the relevant fractions of the total sample volume (Grainger, 1969; Zachariasen & Plettinger, 1965).

On the other hand, it is readily seen that if two reflections coincide, the intensity at the reciprocal-lattice point will be proportional to $|pF_1 + qF_2|^2$. For example, the scattering amplitude for the whole pseudo-crystal is

$$F(\mathbf{u}) = \sum_i F_i \exp(2\pi i \mathbf{u}.\mathbf{R}_i), \qquad (1)$$

where F_i is the scattering amplitude and $\mathbf{R}_i$ is the vector to the origin of the ith unit cell. For a vector $\mathbf{u}$ to a common reciprocal-lattice point, all the exponential factors will be unity so that

$$|F(\mathbf{u})|^2 = |\sum_i F_i|^2 = |pF_1 + qF_2|^2. \qquad (2)$$

The same argument applies to the reciprocal-lattice points of an average lattice in cases when the differences in orientation of the two twin components are very small and the spots overlap but do not coincide.

The result (2) holds in practice only for a coherently diffracting region of the sample. The coherence width of the incident X-ray beam is normally no more than a few hundred ångströms. If the distance between twin planes is much greater than this the single-crystal regions diffract separately and no problem arises. In the presence of microtwinning with twin planes separated by distances comparable with the coherence width, the situation needs to be examined in detail.

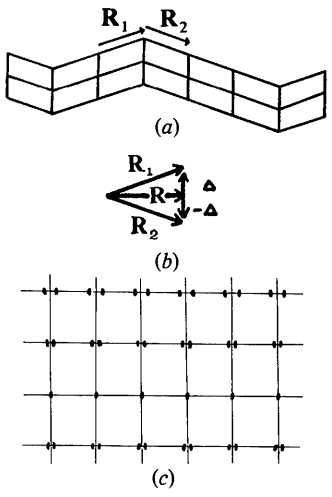

Fig. 1. The model system used as a basis for calculations. In the real-space diagrams (*a*) and (*b*) the angles between the vectors $\mathbf{R}_1$ and $\mathbf{R}_2$ have been exaggerated. Diagram (*c*) shows the pairs of diffraction maxima around the reciprocal-lattice points of the average lattice.

A simple model

We consider the case of two types of layer, one unit-cell thick, for which the layer structure amplitudes are F_1 and F_2 and the repetition vectors are $\mathbf{R}_1$ and $\mathbf{R}_2$. Faults in which one type of layer is followed by the other type occur with a probability α. At the interfaces there is no change in the unit-cell content or repetition vector for either type of layer so that the parameters defined in (I) have values, $\mathbf{S}_{ij} = 0$, $G_{ij} = 0$, $g_i = \frac{1}{2}$, $\alpha_{12} = \alpha_{21} = \alpha = A_i$. Then the general expression of (I) [equation (7)] reduces to

$$\frac{I}{N} = \frac{1}{2}\left\{\sum_{i=1,2} \frac{F_i^*}{1-(1-\alpha)\exp(2\pi i \mathbf{u}.\mathbf{R}_i)} \times \left[F_i + \sum_j \frac{\alpha \exp(2\pi i \mathbf{u}.\mathbf{R}_i)}{1-(1-\alpha)\exp(2\pi i \mathbf{u}.\mathbf{R}_j)} \times [F_j + \cdots]\right] + \text{c.c.} - \sum_{i=1,2} |F_i|^2\right\}. \qquad (3)$$

Writing, for convenience

$$\alpha_i' \equiv \alpha \exp(2\pi i \mathbf{u}.\mathbf{R}_i),$$

$$f_i \equiv 1 - (1-\alpha)\exp(2\pi i \mathbf{u}.\mathbf{R}_i),$$

we obtain

$$\frac{2I}{N}(\mathbf{u}) = \sum_{i=1,2}\left\{\frac{F_i^*}{f_i}\left[F_i + \frac{\alpha_i'}{f_j}\left[F_j + \frac{\alpha_j'}{f_i}\left[F_i + \cdots\right]\right]\right] + \text{c.c.} - |F_i|^2\right\}$$

$$= \frac{f_2|F_i|^2 + f_1|F_2|^2 + \alpha_1' F_1^* F_2 + \alpha_2' F_1 F_2^*}{(f_1 f_2 - \alpha_1'\alpha_2')} + \text{c.c.} - |F_1|^2 - |F_2|^2. \qquad (4)$$

For the simple case of microtwinning illustrated in Fig. 1 with a small angle between the vectors $\mathbf{R}_1$ and $\mathbf{R}_2$, we define an average repetition vector $\mathbf{R}$ and put (Fig. 1*b*)

$$\mathbf{R}_1 = \mathbf{R} + \boldsymbol{\Delta}, \quad \mathbf{R}_2 = \mathbf{R} - \boldsymbol{\Delta}.$$

The reciprocal-space representation, Fig. 1(*c*), shows the reciprocal lattices for the two crystals considered separately (large distances between twin planes). Around each reciprocal-lattice point $\mathbf{h}$ for the average lattice there is a pair of spots at $\mathbf{h} \pm \boldsymbol{\varepsilon}$ with the vector $\boldsymbol{\varepsilon}$ perpendicular to $\boldsymbol{\Delta}$ and of magnitude $|\boldsymbol{\varepsilon}| = (\mathbf{h}.\boldsymbol{\Delta})/R$.

If the probability of twinning is appreciable, the pairs of spots will tend to merge into streaks along the layer line. We can then calculate the intensity for microtwins by considering the intensity as a function of $\mathbf{u} = \mathbf{h} + \boldsymbol{\varepsilon}$ where $|\boldsymbol{\varepsilon}|$ is a continuous variable or, to use fractional coordinates, we plot $I(u)$ for values of $(\mathbf{u} - \mathbf{h}).\mathbf{R} = \boldsymbol{\varepsilon}.\mathbf{R} = \varepsilon R$.

For this case (4) may be written

$$\begin{aligned}\frac{I}{N}(u) = \alpha(1-\alpha)[&|F_1|^2\{1-\cos 2\pi\mathbf{u}.(\mathbf{R}-\boldsymbol{\Delta})\}\\ &+|F_2|^2\{1-\cos 2\pi\mathbf{u}.(\mathbf{R}+\boldsymbol{\Delta})\}\\ &+2\{A_1A_2+B_1B_2)\cos 2\pi\mathbf{u}.\boldsymbol{\Delta}\\ &+(A_1B_2-A_2B_1)\sin 2\pi\mathbf{u}.\boldsymbol{\Delta}\}(\cos 2\pi\mathbf{u}.\mathbf{R}\\ &-\cos 2\pi\mathbf{u}\boldsymbol{\Delta})][\alpha^2\sin^2 2\pi\mathbf{u}.\mathbf{R}+(1-\alpha)^2\\ &\times(\cos 2\pi\mathbf{u}.\mathbf{R}-\cos 2\pi\mathbf{u}.\boldsymbol{\Delta})^2]^{-1}, \qquad (5)\end{aligned}$$

where we have put $F_i = A_i + iB_i$.

Analysis of this expression readily reveals that it has the expected behavior in the limiting cases. Thus for α tending to zero we have delta-function peaks for $\mathbf{u}.\mathbf{R} = \pm\mathbf{u}.\boldsymbol{\Delta}$ of weight $|F_1|^2$ and $|F_2|^2$. For a reciprocal-lattice point of the average lattice, $\varepsilon = 0$, $\cos 2\pi\mathbf{u}.\mathbf{R} = 1$, the intensity is proportional to $|F_1 + F_2|^2$ if $\mathbf{u}.\boldsymbol{\Delta}$ is small.

For the case $\boldsymbol{\Delta} = 0$ with unit cells of identical dimensions but differing in content, (5) reduces to (apart from a delta function at the reciprocal-lattice point)

$$\frac{2I(u)}{N} = \frac{\alpha}{1-\alpha}\,\frac{2|F_1 - F_2|^2}{\{4\alpha^2 + (1-\alpha)^2(2\pi\varepsilon R)^2\}}$$

if εR is small so that there is a diffuse peak of half width $2\pi\varepsilon R = 2\alpha/(1-\alpha)$.

In general, the spreading of the peaks along the layer line due to the disordered streaking will be comparable to the separation of the pairs of spots due to twinning if $2\pi\mathbf{h}.\boldsymbol{\Delta} \simeq 2\alpha/(1-\alpha)$. For larger values of $\mathbf{h}.\boldsymbol{\Delta}$ two distinct reflections will be seen. For smaller values of $\mathbf{h}.\boldsymbol{\Delta}$ there will be only a single intensity maximum.

The expression (5) can be integrated analytically over one reciprocal-lattice periodicity. The integrated intensity is always proportional to $|F_1|^2 + |F_2|^2$, independent of the magnitudes of $\boldsymbol{\Delta}$ and α.

The question remains as to whether the intensity of the peak or peaks which would be measured using the standard techniques of X-ray diffraction, which involve a certain amount of integration, would also be proportional to $|F_1|^2 + |F_2|^2$. In order to estimate the magnitude of any possible errors in this assumption we have calculated intensity curves using (5) for various values of $\mathbf{h}.\boldsymbol{\Delta}$ and α which seemed appropriate.

Estimation of measured intensities

In diffractometer measurements of X-ray diffraction peak intensities it is customary to use either an ω scan or a θ–2θ scan over an angular range of 1·4 or 2°, which is normally sufficient to establish a background value on either side of the peak and to integrate over the peak which has a width of 1° or less due to incident-beam divergence and mosaic spread. A spreading of the peaks by an amount 2×10^{-2} rad by the effect of disordered stacking is therefore about the maximum which would allow the standard measurement routines to be used.

For a value of $2\alpha/(1-\alpha) = 0{\cdot}1$ with a repetition distance R of 10Å the spreading of the peak is given by $2\pi\varepsilon = 10^{-2}$Å^{-1}. For a reciprocal-lattice point at a distance 1Å^{-1} from the origin the angle subtended by the half width of the peak is 3×10^{-3} rad. Hence, if we take $\alpha = 0{\cdot}05$, so that the average distance between twin planes is 20 unit cells, the spreading of the peaks due to the microtwinning disorder will be less than that due to beam convergence and mosaic spread and will not normally be distinguishable from these effects.

We have calculated intensity profiles for diffraction peaks for $\alpha = 0{\cdot}05$ and for $2\pi\mathbf{h}.\boldsymbol{\Delta}$ values of 0·025, 0·05 and 0·10. For the smallest of these $\mathbf{h}.\boldsymbol{\Delta}$ values the separation of the pair of peaks due to twinning is considerably less than the spread due to α so that only a single peak will be observed. For the largest $\mathbf{h}.\boldsymbol{\Delta}$ value the pair of peaks is separated although it is not clear whether the two peaks will be observed and measured separately in normal X-ray diffraction experiments. The value, $2\pi\mathbf{h}.\boldsymbol{\Delta} = \alpha$, is intermediate.

In Fig. 2 the intensity profiles calculated for $\alpha = 0{\cdot}05$ and the above mentioned values of $2\pi\mathbf{h}.\boldsymbol{\Delta}$ are plotted for various values of the ratio F_1/F_2 ranging from 1 to -1. For convenience F_1 and F_2 are assumed to be real. Calculations for complex F_1 and F_2 show much the same behaviour.

For $2\pi\mathbf{h}.\boldsymbol{\Delta} = \alpha/2$ and F_1, F_2 of the same sign, a single relatively sharp peak is seen. For F_1 and F_2 of opposite sign there is a sharp minimum in the peak. As expected, this is zero at the reciprocal-lattice point, $\varepsilon = 0$, for $F_1 + F_2 = 0$. However, this minimum is so sharp that it is unlikely to be observed in practice.

For $2\pi\mathbf{h}.\boldsymbol{\Delta} = 0{\cdot}1$ the minimum may well be so pronounced and broad for F_1 and F_2 of opposite sign that two distinct peaks may be observable in practice, although for F_1 and F_2 of the same sign the separation is not so distinct. In general, the intensity peaks are seen to be symmetrical only for $F_1/F_2 = \pm 1$. The asymmetry for other cases derives from the $\sin 2\pi\mathbf{u}.\mathbf{R}$ terms which occur in the expansion of the numerator of (5).

Since integration of the intensity curves gives a value proportional to $|F_1|^2 + |F_2|^2$ in every case, the possible error in assuming this value for the measured intensity comes from the difficulty of measuring the total intensity under the curves of Fig. 2. The difficulty arises because an appreciable part of the intensity is contained in the long tails of the peaks extending to $\varepsilon R =$

± 1, *i.e.* from one reciprocal-lattice point to the next. There will be, in general, no way in which these long tails can be separated from background scattering due to residual white radiation, thermal diffuse scattering or other causes. The asymmetry of the tails for $F_1/F_2 \neq \pm 1$ will not usually help the separation because asymmetries in background due to other causes are not usually determined quantitatively.

In order to estimate the errors which may result from the neglect of these long tails on the intensity peaks, we have drawn in Fig. 2 with dashed lines the values which may be assumed for the background under the peaks if the tails due to the disorder are not distinguished from other background contributions. In the usual diffractometer measuring routine a background count is made at either end of the 1·4 or 2° scan and the background is assumed to be given by a straight-line interpolation between these two points. If the end points of the scan are obviously high on the sides of the peak and clearly not in the background region, the measurement will

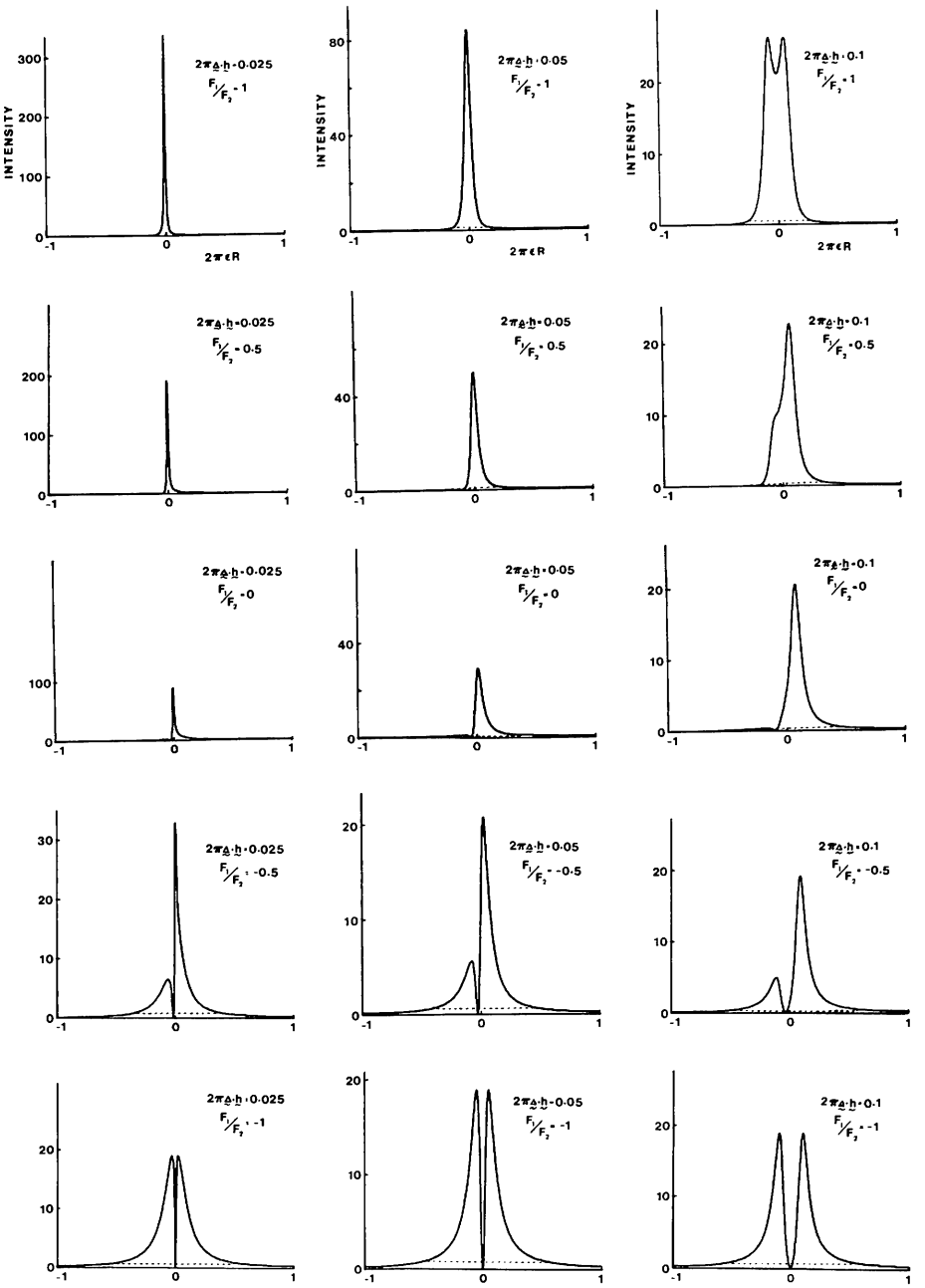

Fig. 2. Intensity profiles of diffraction maxima calculated for $\alpha = 0{\cdot}05$ and the indicated values of $2\pi\mathbf{h}.\boldsymbol{\Delta}$ and the ratios of structure amplitudes.

presumably be rejected and repeated with a wider scan. Hence the backgrounds which we have indicated in Fig. 2 correspond to something like the highest values which would be measured for any scan width.

The actual points at which the background measurements would be made on the plots of Fig. 2 will depend strongly on the geometry of measurement. The measured intensity for each diffractometer position is given by the integration of the product of the scattering power distribution with the detector function, which may be represented to a first approximation by a volume in reciprocal space of uniform detector sensitivity, as illustrated in Fig. 3. The measurement of a peak intensity is made by translating this volume over the reciprocal-lattice point by either a θ–2θ or an ω scan. The actual distance in terms of $2\pi\varepsilon R$ which is covered by a 1·4 or 2° scan will then depend on the distance of the reciprocal-lattice point from the origin, $d_{\mathbf{h}}^{-1}$, the angle between the directions of the θ–2θ or ω scans with the layer lines and the unit-cell dimension, R. In some scan directions, as in the case of a θ–2θ scan with the short axes of the measuring volume nearly perpendicular to the streaked layer lines of Fig. 1(*c*), the measuring volume will not intersect the elongated spots at either end of the scan. Then the distance in $2\pi\varepsilon R$ over which the integration of intensity will be made will depend on the long dimension of the measuring volume, defined by the detector angle β which is usually about 1·5°.

If we take 1·5° as either the scan length or the value of angle β, whichever is relevant, we see that for R = 10 Å the corresponding minimum range of $2\pi\varepsilon R$ is 0·32 for $d_{\mathbf{h}}^{-1} = 0{\cdot}2$ Å^{-1} and 1·6 for $d_{\mathbf{h}}^{-1} = 1$ Å^{-1}. The ranges of $2\pi\varepsilon R$ for which we have assumed the peaks to exceed background vary from 0·25 to about 0·75. Hence, our estimates of error will represent the maximum error which may be introduced for some particular $d_{\mathbf{h}}^{-1}$ and R values but may be considerable overestimates for other conditions. They are therefore to be taken as rough indications of the upper limits of possible error.

On the basis of the background assumptions indicated in Fig. 2, the maximum errors made in assuming the integrated intensities to be proportional to $|F_1|^2 + |F_2|^2$ are as indicated in Fig. 4. The errors are seen to be 30 to 40% for F_1 and F_2 of opposite sign, decreasing to 0 to 5% for F_1 and F_2 of the same sign and almost equal. The errors are less for smaller values of $\mathbf{h}.\boldsymbol{\Delta}$ but, as seen from the form of (6), will not be zero for $\mathbf{h}.\boldsymbol{\Delta} = 0$.

It is to be expected that for $\alpha = 0$ there will be just two sharp peaks having intensities $|F_1|^2$ and $|F_2|^2$. In order to find the dependence on α we have made calculations for $\alpha = 0{\cdot}2$ and $\alpha = 0{\cdot}02$ with $\mathbf{h}.\boldsymbol{\Delta} = \alpha$ in each case. For $\alpha = 0{\cdot}2$ the error curve was identical with the $\alpha = 0{\cdot}05 = \mathbf{h}.\boldsymbol{\Delta}$ curve of Fig. 2 within the broad limits of error of our rough estimations. With $\alpha = 0{\cdot}02 = 2\pi\mathbf{h}.\boldsymbol{\Delta}$ the maximum errors were found to be roughly $\frac{3}{4}$ of those for $\alpha = 0{\cdot}05 = 2\pi\mathbf{h}.\boldsymbol{\Delta}$. On the other hand, since the spread of the peaks is less for the lower α value the maximum error values will occur less often, being restricted to smaller $d_{\mathbf{h}}^{-1}$ and R values. However, it appears that appreciable errors are possible even for very small values of α corresponding to twin planes spaced at intervals of 50 to 100 unit cells.

Conclusions

Our analysis has indicated that for microtwins the fact that the intensity at the reciprocal-lattice point is proportional to $|F_1 + F_2|^2$ is scarcely relevant. The integration over angle which is unavoidable in normal intensity measurement procedures will give a result more nearly proportional to $|F_1|^2 + |F_2|^2$ except when the degree of disorder is so great that the usual procedures would clearly be inappropriate.

The main source of error in the assumption that the integrated intensity is proportional to $|F_1|^2 + |F_2|^2$ comes from the difficulty of including the long tails of the intensity peaks in the measurement. From the curves of Fig. 2 it is seen that these tails are present whether the peak is resolved into two components or not. The form of the intensity maxima is such that up to one third of the intensity may be contained in these

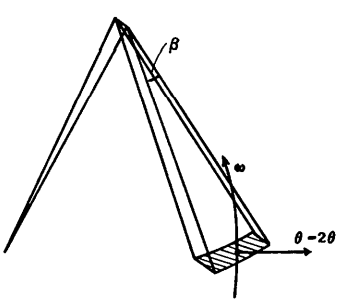

Fig. 3. Diagram of the measuring volume in reciprocal space and its motions for an ω scan and a θ–2θ scan.

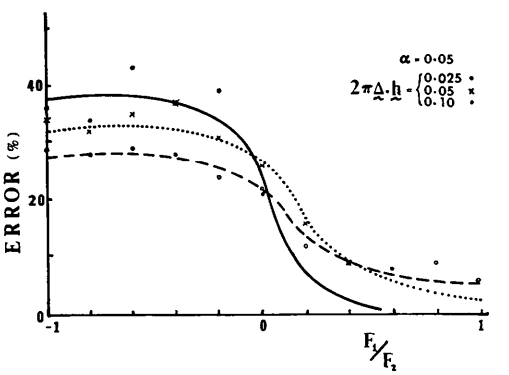

Fig. 4. Estimated maximum errors of intensity measurement as a function of the ratio of structure amplitudes.

long tails which may not be distinguishable from background scattering due to other sources.

Our estimates of error from this source are admittedly very rough and subjective and are intended only as indications of the possible magnitudes of the errors and their variation with the relevant parameters. The actual errors of measurement will depend on a number of factors. The curves of Fig. 2 will be convoluted in practice with an instrumental measuring function and a mosaic spread function which will vary in width and form with the distance of the reciprocal-lattice point from the origin and also with the angle between the **h** vector and the repetition vector **R**. The estimates of background will depend on the measuring routine used.

In the reciprocal-space representation of Fig. 1(*c*) it is seen that for our simple model the value of $\mathbf{h}.\Delta$ is zero on one line through the origin and varies systematically with distance from this line. Since from Fig. 4 it is seen that there is only a weak dependence of the error on $\mathbf{h}.\Delta$, the effect will be to produce only a small systematic variation of measured intensity. However, the variation of the form and size of the measuring volume in reciprocal space (Fig. 3) will tend to give a larger systematic error with position of the reciprocal-lattice point since the varying range of measurement in terms of $2\pi\varepsilon R$ will give an error ranging from almost zero to the maximum indicated in Fig. 4.

In general, the errors in relative intensities will be less if F_1 and F_2 are of the same sign and differ by less than 50%. It is for the occasional pairs of reflections for which F_1 and F_2 have opposite sign that the relatively large errors may be produced.

It is suggested that when microtwinning is indicated by streaking in X-ray diffraction or electron diffraction patterns or by contrast effects in high-resolution electron micrographs (Wenk, 1976) estimates may be made of the possible errors on the basis of the above considerations in relation to the techniques used for measurement of X-ray diffraction intensities. In this way improved accuracy may be obtained in structure analyses when microtwinning is present.

The authors are grateful to Drs Gabrielle and J. D. H. Donnay for stimulating discussions in the initiation of this project and in review of the manuscript, and also to Dr R. Von Dreele for advice on diffractometer measuring techniques. The work was supported by NSF grant DMR 76-06108.

References

COWLEY, J. M. (1976*a*). *Acta Cryst.* A**32**, 83–87.
COWLEY, J. M. (1976*b*). *Acta Cryst.* A**32**, 88–91.
GRAINGER, C. T. (1969). *Acta Cryst.* A**25**, 427–434.
IIJIMA, S. & BUSECK, P. R. (1976). *Electron Microscopy in Mineralogy*, edited by H.-R. WENK, pp. 319–323. Heidelberg: Springer.
MCLAREN, A. C. & MARSHALL, D. B. (1974). *Contrib. Mineral. Petrol.* **44**, 237–249.
PRINCE, E., DONNAY, G. & MARTIN, R. F. (1973). *Am. Mineral.* **58**, 500–507.
WENK, H.-R. (1976). *Electron Microscopy in Mineralogy*. Heidelberg, New York: Springer.
ZACHARIASEN, W. H. & PLETTINGER, H. A. (1965). *Acta Cryst.* **18**, 710–716.

Acta Cryst. (1978). A**34**, 743–746

Minimizing the Variance in Integrals and Derivatives of the Electron Density

BY C. L. DAVIS AND E. N. MASLEN

Department of Physics, University of Western Australia, Nedlands, Western Australia

(*Received* 21 *November* 1977; *accepted* 28 *March* 1978)

A method for minimizing the variance in integrals and derivatives of electron densities by filtering the scattering amplitudes is established. The optimum filters for the density and its integrals and derivatives are shown to be the same. Calculations with experimental data show that the variance of integrated densities is not very sensitive to the shape of the region of integration, indicating that good estimates may be made using simple shapes. A very convenient expression is given for the variance of the integral over a sphere. Coppens & Hamilton [*Acta Cryst.* (1968), B**24**, 925–929] have shown that accurate estimates of integrated densities are possible. Filtering can further improve these estimates. By contrast, good estimates of derivatives of the electron density remain unlikely, even using filtered diffraction data.

Introduction

In quantitative studies of the structure of materials by the analysis of diffraction data it is often of interest to calculate gradients and volume integrals of the electron density. When the density is evaluated by Fourier synthesis of the structure factors, **F**(**S**) (**S** is the reciprocal-lattice vector), difficulties arise in the treatment of the